Article

Theoretical Investigations on Donor−Acceptor Conjugated Copolymers Based on Naphtho[1,2-c:5,6-c]bis[1,2,5]thiadiazole for Organic Solar Cell Applications

Linghai Zhang,[‡] Ke Pei,[‡] Mudan Yu,[‡] Yuanling Huang,[‡] Hongbo Zhao,[†] Min Zeng,[‡] Yang Wang,[‡] and Jinwei Gao[‡,*]

[‡]Institute of Advanced Material (IAM), Academy of Advanced Optoelectronics, South China Normal University, Guangzhou 510006, China

[†]School of Physics and Telecommunication Engineering, South China Normal University, Guangzhou 510006, China

ABSTRACT: Conjugated polymers with donor−acceptor architectures have been successfully applied in bulk hetero-junction solar cell devices. Tuning the electron-withdrawing capability in donor−acceptor (D−A) conjugated polymers allows for design of new polymers with enhanced electrical and optical properties. In this paper, a series of D−A copolymers, PBDFDTBT (P1a), PBDTDTBT (P2a), PNDTDTBT (P3a), and PQDTDTBT (P4a), were selected and theoretically investigated using PBE0/6-311G** and TD-PBE0/6-311G**//PBE0/6-311G** methods. The calculated results agree well with the available experimental data of HOMO energy levels and band gaps. We further designed and studied four novel copolymers, P1b, P2b, P3b, and P4b, by substituting the 2,1,3-benzothiadiazole (BT) unit in P1a−P4a with a stronger unit of naphtho[1,2-c:5,6-c]bis[1,2,5]thiadiazole (NT), respectively. Compared with P1a−P4a, the newly designed polymers of P1b−P4b show better performance with the smaller band gaps and lower HOMO energy levels. The PCEs of ∼5%, ∼7%, ∼7%, and ∼7% for P1b−P4b, predicted by Scharber diagrams, are much higher than those of P1a−P4a when used in combination with PCBM. These results clearly reveal that tuning the electron-withdrawing capability in D−A conjugated polymers is an effective way to improve the electrical and optical properties and the efficiency of the photovoltaic device.
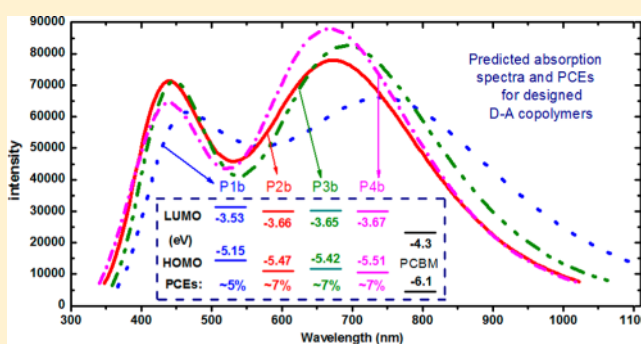
1. INTRODUCTION

Polymer solar cells (PSCs) have attracted increasing attention in recent years due to their several advantages, such as low cost, flexibility, lightweight, solution-based processing, and large-area devices.[1−5] The typical conjugated conducting polymers have been extensively scrutinized and successfully applied in bulk heterojunction (BHJ) solar cell devices.[5,6] Among the conjugated polymers, the concept of the donor−acceptor (D−A) copolymer has been widely adopted for design of a donor polymer with a narrow band gap.[7,8] In the past years, the power conversion efficiencies (PCEs) of solar cells with such configurations have improved from ∼1% to ∼9%.[5,9]

It is well-known that, to obtain a high PCE, both the band gap and the orbital energy levels of a donor polymer should be optimized simultaneously.[10,11] In general, the key strategies to improve the efficiency of organic solar cells include the following: (1) reducing the highest occupied molecular orbital (HOMO) energy level of a molecule (generally for donor) provides a large open circuit voltage (V_{oc});[3] (2) decreasing the band gap of a molecule creates a high short-circuit current density (J_{sc});[12] (3) moreover, maintaining at least an energy difference of 0.3 eV between the lowest unoccupied molecular orbitals (LUMOs) of a donor and an acceptor to ensure the

maximum charge separation at the donor/acceptor inter-face.[13,14] Besides, high charge carrier mobility, high solubility for solution processing in fabrication of the bulk heterojunction PSCs, optimal morphology, and nanoscaled phase separation of the interpenetrating network of the donor/acceptor blend in the active layer are also required in the molecular design of the high efficiency photovoltaic materials.[5,8]

In experiment, the optical band gap (E^{opt}) is measured by UV/vis absorption, and the HOMO energy level is obtained by cyclic voltammetry (CV) or ultraviolet photoelectron spectros-copy (UPS).[15] The LUMO energy level is subsequently estimated from the equation, $E_{LUMO} = E_{HOMO} + E^{opt}$.[15−18] A quantum-chemical technique, a reliable and accurate method, has been widely used to explain and predict orbital energy levels and band gaps of molecules, especially unknown conjugated polymers.[19−23] It is generally accepted that the oligomer method offers a reasonable result of the band gap by extrapolating the y intercept from the linear fit of the LUMO−HOMO gap against the reciprocal of the number of monomer

A

units $(1/n)$.[23−25] However, in terms of computational cost, it is difficult to use this approach for those polymers in which the repeating units contain too many atoms. Recent studies[19,21,22,26] showed that the predicted band gaps and HOMO energy levels based on both the monomer and the dimer models, calculated by the DFT method with some specific basis sets, agree well with the experimental data. For example, Xiao and Liu et al.[19] showed that the most accurate HOMO energy level of a polymer was predicted by the B3LYP/6-311+G(d) method with a monomer model. Very recently, Ku and co-workers[21] have revealed that the calculations by DFT combined with TDDFT at B3LYP/6-311G(d,p) with a dimer model can reproduce the experimental HOMO/LUMO levels and the band gaps of push−pull-type copolymers. TD-PBE0 has also shown its outperformance in the calculations of excitation energies of organic molecules.[27−29] Thus, the methods of (TD) DFT with an appropriate basis set on the monomer or the dimer model are reliable and direct ways to calculate the band gaps and the HOMO energy levels of polymers, which are the most critical parameters for determining the solar cell efficiency.

2,1,3-Benzothiadiazole (BT) is one of the most accepted acceptor units in constructing a low band gap conjugated donor polymer due to its strong electron-withdrawing capability and commercial availability.[6] However, recently, a kind of new NT-based (NT, naphtho[1,2-c:5,6-c]bis[1,2,5]thiadiazole) polymer has been reported and applied in solar cell devices with considerably high J_{sc} and significantly good photovoltaic performance because the unit of NT has a much stronger electron-withdrawing capability than BT.[30−32]

In this paper, four D−A copolymers[33−35] (PBDFDTBT (P1a or $(1a)_n$), PBDTDTBT (P2a or $(2a)_n$), PNDTDTBT (P3a or $(3a)_n$), and PQDTDTBT (P4a or $(4a)_n$) (in Figure 1a), which contain a dithienylylbenzothiadiazole (DTBT) acceptor unit and different donor units of benzo[1,2-b:4,5-b′]difuran[33] (BDF), benzo[1,2-b:4,5-b′]dithiophene[34] (BDT), naphtho-[2,1-b:3,4-b′]dithiophene[35] (NDT), and dithieno[3,2-f:2′,3′-h]quinoxaline[35] (QDT), were calculated on the HOMO energy levels and the band gaps by a theoretical quantum-chemical method. On the basis of these calculated results, we hence replaced BT with NT in P1a, P2a, P3a, and P4a, respectively, and designed four new D−A copolymers. These designed polymers (as shown in Figure 1a) of PBDFDTNT (P1b), PBDTDTNT (P2b), PNDTDTNT (P3b), and PQDTDTNT (P4b) were theoretically investigated using the same methods on the structures, orbital energy levels, band gaps, and optical spectra. The results show that these NT-based polymers possess lower band gaps, deeper HOMO energy levels, and better predicted photovoltaic performances than BT-based polymers, which reveals that the method of tuning the electron-withdrawing capability of donors is an efficient way to improve the performance of the D−A conjugated polymers.

2. COMPUTATIONAL DETAILS

All the quantum chemistry calculations were carried out in the Gaussian 03 package.[36] The ground-state geometries of oligomers were fully optimized using the density functional theory (DFT).[37] To simplify the calculation, all alkyl-branched chains (R_1 and R_2, shown in Figure 1a) were replaced by methyl groups, and the terminals of the repeating units were saturated with hydrogen atoms.[21]

To find the appropriate method, P1a−P4a were calculated at the different functionals (B3P86, BPBE,[38] B3LYP,[39,40] PBE0,[41]
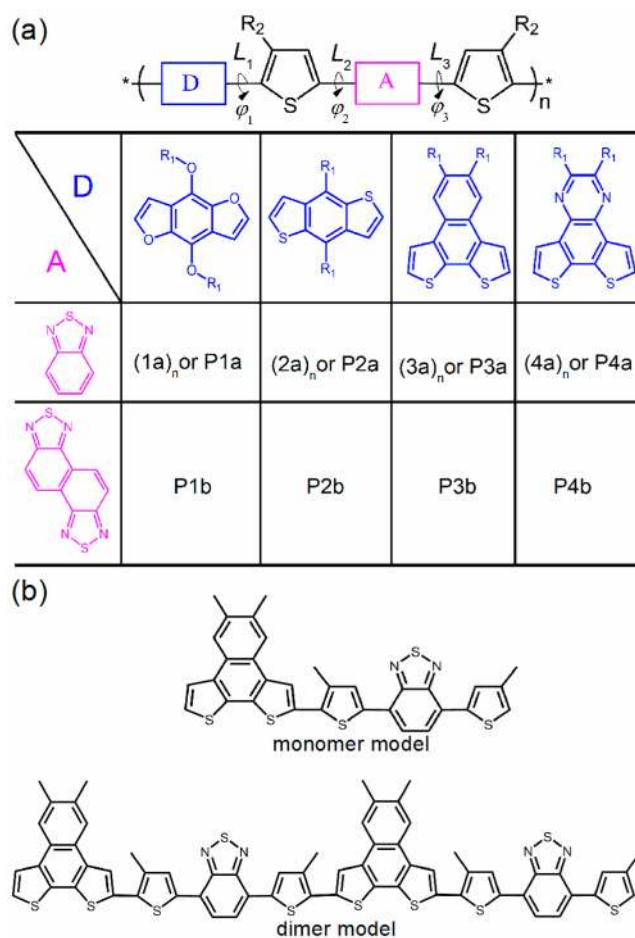
Figure 1. (a) Molecular structures of BT-based and NT-based copolymers by combinations of different donors ('D') and different acceptors ('A') shown in the table, respectively. The R_1 and R_2 shown in molecular structures are alkyl-branched chains. (b) Samples of the two calculated models: the monomer and dimer models. In the monomer or dimer structures, the R_1 and R_2 groups have been replaced with a methyl group.

and BHandHLYP[42]) with a 6-311G** basis set (on the monomer model); also, the HOMO energy levels were predicted. We used two methods to calculate the band gaps for polymers. The first method is oligomer approach by extrapolating the y intercept from the linear fit of the LUMO−HOMO gap ($\Delta E_{\text{LU-HO}}$: the difference between the LUMO and HOMO energy level, at the B3LYP/6-31G* level) against the reciprocal of the number of monomer units $(1/n)$. Another is to directly calculate the band gaps of polymers by time-dependent DFT (TDDFT)[43−46] (PBE0 functional) with different basis sets (3-21G*, 6-31G*, 6-311G**) with a dimer model (as shown in Figure 1b). The LUMO energy levels were estimated from the equation,[21] $E_{\text{LUMO}} = E_{\text{HOMO}} + E_{\text{g,TD}}$. A similar strategy has been used in previous experiments ($E_{\text{LUMO}} = E_{\text{HOMO}} + E^{\text{opt}}$).[15−18] The absorption spectra were predicted by the TD-PBE0/6-311G**//PBE0/6-311G** method with a dimer model. All calculations were performed without any symmetry constraints and only in the gas phase.

3. RESULTS AND DISCUSSION

3.1. Choice of Method for the HOMO Energy Level Calculations. To find an appropriate functional for the calculations of HOMO energy levels of polymers, we chose a

Table 1. HOMO Energy Levels (in eV) of M1a–M4a Obtained in the Gas Phase with Different Functionals at the 6-311G** Level

oligomer	BPBE	B3LYP	PBE0	BHandHLYP	B3P86	exp. (polymer)
M1a	−4.27	−4.94	−5.10	−5.82	−5.55	−5.10[a]
M2a	−4.60	−5.24	−5.40	−6.13	−5.83	−5.40[b]
M3a	−4.58	−5.21	−5.37	−6.09	−5.81	−5.34[c]
M4a	−4.67	−5.29	−5.46	−6.17	−5.89	−5.46[c]

[a]From ref 33. [b]From ref 34. [c]From ref 35

Table 2. HOMO and LUMO Energy Levels and LUMO−HOMO Gaps ($\Delta E_{\text{LU-HO}}$) (in eV) of $(1a)_n$, $(2a)_n$, $(3a)_n$, and $(4a)_n$ ($n = 1–3, \infty$) at the B3LYP/6-31G* Level[a]

| oligomer	E_{LUMO}	E_{HOMO}	$\Delta E_{\text{LU-HO}}$	exp.	oligomer	E_{LUMO}	E_{HOMO}	$\Delta E_{\text{LU-HO}}$	Exp.
$(1a)_n$					$(2a)_n$				
$n = 1$ (M1a)	−2.62	−4.71	2.09	-	$n = 1$ (M2a)	−2.66	−4.98	2.32	-
$n = 2$ (D1a)	−2.76	−4.65	1.89	-	$n = 2$ (D2a)	−2.77	−4.81	2.04	-
$n = 3$ (T1a)	−2.80	−4.62	1.82	-	$n = 3$ (T2a)	−2.82	−4.77	1.95	-
$n = \infty$	-	-	1.69	1.85−2.02[b]	$n = \infty$	-	-	1.76	1.77−1.98[c]
$(3a)_n$					$(4a)_n$				
$n = 1$ (M3a)	−2.64	−4.93	2.29	-	$n = 1$ (M4a)	−2.66	−5.02	2.36	-
$n = 2$ (D3a)	−2.75	−4.73	1.98	-	$n = 2$ (D4a)	−2.78	−4.82	2.04	-
$n = 3$ (T3a)	−2.80	−4.68	1.88	-	$n = 3$ (T4a)	−2.82	−4.77	1.95	-
$n = \infty$	-	-	1.67	1.82−1.97[d]	$n = \infty$	-	-	1.74	1.92−2.04[d]

[a]Here, "M", "D", and "T" denote monomer, dimer, and trimer, respectively. [b]From ref 33. [c]From ref 34. [d]From ref 35

wide class of functionals from pure (BPBE) to hybrid functionals including B3LYP, PBE0, BHandHLYP, and B3P86 at 6-311G** on a monomer model. As shown in Table 1, the calculated results of the HOMO energy levels at the PBE0/6-311G** level (−5.10, −5.40, −5.37, and −5.46 eV for M1a, M2a, M3a, and M4a, respectively; here "M" means monomer) agree well with the experimental data of polymers (−5.10,[33] −5.40,[34] −5.34, and −5.46 eV[35] for P1a, P2a, P3a, and P4a, respectively). By comparison, the calculations by other functionals deviate more from the experiments. For example, the BPBE/6-311G** method (−4.27, −4.60, −4.58, and −4.67 eV for M1a, M2a, M3a, and M4a, respectively) tends to overestimate the experimental HOMO energy levels of these polymers, while the calculations at the B3P86/6-311G** level (−5.55, −5.83, −5.81, and −5.89 eV for M1a, M2a, M3a, and M4a, respectively) tend to underestimate those experimental data. Thus, we implemented the following HOMO energy level calculations at the PBE0/6-311G** level.

3. 2. Comparison between Theoretical and Experimental Band Gaps.

It is generally accepted that the band gaps of conjugated polymers can be extrapolated to the y intercept from the linear fit of $\Delta E_{\text{LU-HO}}$ against the reciprocal of the number of monomer units $(1/n)$.[23] The method of DFT/B3LYP/6-31G* has been believed to be an accurate and reliable formalism to predict the band gaps of a molecule.[13] In this paper, B3LYP/6-31G* is also used to investigate the $\Delta E_{\text{LU-HO}}$ of the oligomers of $(1a)_n$, $(2a)_n$, $(3a)_n$, and $(4a)_n$ with $n = 1, 2,$ and 3, respectively. The band gaps of corresponding polymers are produced by extrapolating the y intercept from the plot of $\Delta E_{\text{LU-HO}}$ with $1/n$.

Table 2 shows the calculated HOMO and LUMO energy levels and LUMO−HOMO gaps of $(1a)_n$, $(2a)_n$, $(3a)_n$, and $(4a)_n$ ($n = 1–3, \infty$) at the B3LYP/6-31G* level, along with the experimental data.[33–35] With increasing conjugation lengths, the HOMO and LUMO energy levels change with the opposite direction, which gradually narrows the band gaps of all oligomers. The extrapolated band gaps (in Table 2 and Figure 2) show the $\Delta E_{\text{LU-HO}}$ of $(1a)_n$, $(2a)_n$, $(3a)_n$, and $(4a)_n$ are 1.69, 1.76, 1.67, and 1.74 eV, respectively. The experimental E^{opt} are
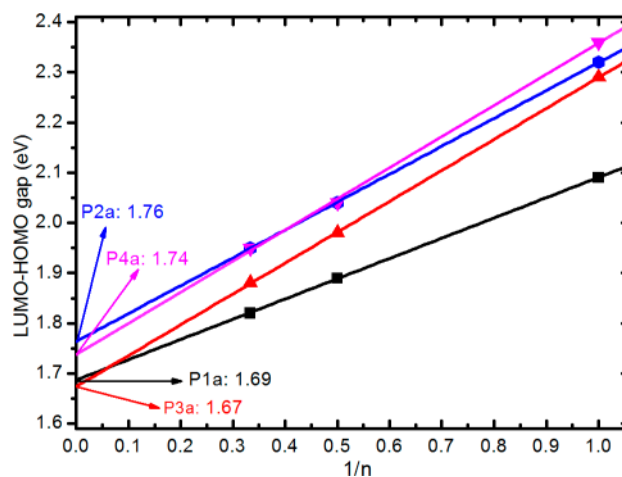
Figure 2. LUMO−HOMO gaps (at the B3LYP/6-31G* level) versus the reciprocal of the number of oligomer units for P1a, P2a, P3a, and P4a, along with the band gaps from extrapolating the y intercept when $1/n$ equals 0.

estimated from the peak maxima in the UV/visible spectra.[17,21] The differences of the band gaps between the experiments (1.85−2.02 eV[33] for P1a, 1.77−1.98 eV[34] for P2a, 1.82−1.97 eV[35] for P3a, and 1.92−2.04 eV[35] for P4a) and the calculations are almost in the range of 0.1−0.4 eV. Obviously, the extrapolated predictions in this calculation far underestimate the experimental band gaps. Also, the calculations of HOMO energy levels (at the B3LYP/6-31G* level, on monomer, dimer and, trimer models) all overestimate those experimental values (the predictions are shown in Table 2, and the experimental data are shown in Table 1), while the predictions of HOMO energy levels by the PBE0/6-311G** method on the monomer model, shown in Table 1, agreed well with the experiments.

Table 3. Vertical Transition Energies and the Corresponding Wavelength of S_1, $E_{g,TD}$ (in eV), and λ_{max} (in nm), of D1a–D4a (Here "D" Denotes Dimer) Obtained in the Gas Phase with the TD-PBE0//PBE0 Method at Different Basis Sets

| oligomer	3-21G*		6-31G*		6-311G**		Exp.(polymer)	
	$E_{g,TD}$	λ_{max}	$E_{g,TD}$	λ_{max}	$E_{g,TD}$	λ_{max}	E^{opt}	λ_{max}
D1a	1.77	699	1.78	698	1.78	698	1.85–2.02[a]	613, ~670[a]
D2a	1.88	659	1.91	648	1.95	637	1.77–1.98[b]	~625, ~700[b]
D3a	1.84	673	1.85	670	1.88	659	1.82–1.97[c]	629, 681[c]
D4a	1.88	658	1.90	652	1.94	638	1.92–2.04[c]	609, 647[c]

[a]From ref 33. [b]From ref 34. [c]From ref 35.

The TDDFT (TD-PBE0) method on the dimer model has also been directly used to calculate and estimate polymer band gaps. To choose an appropriate basis set to predict the band gaps of these polymers, three kinds of basis sets of 3-21G*, 6-31G*, and 6-311G** are applied in these calculations. As listed in Table 3, among those methods, the TD-PBE0/6-311G**//PBE0/6-311G** approach (1.78, 1.95, 1.88, and 1.94 eV for D1a, D2a, D3a, and D4a, respectively) reproduces the experimental band gaps very well. Meanwhile, the corresponding calculated λ_{max} (698, 637, 659, and 638 nm for D1a, D2a, D3a, and D4a, respectively) are also approximately equal to the experimental λ_{max} (613, ~670 nm[33] for P1a; ~625, ~700 nm[34] for P2a; 629, 681 nm[35] for P3a; and 609, 647 nm[35] for P4a). Compared with the extrapolation method, in this paper, direct calculations of the band gaps by the TD-PBE0/6-311G**//PBE0/6-311G** approach are simpler, cheaper, and accurate. Therefore, we conducted the following band gap calculations and discussions using the TD-PBE0/6-311G**//PBE0/6-311G** method with a dimer model.

In addition, the periodic boundary conditions (PBCs) approach also has been shown to be a very good method to reliably predict the band gaps of conjugated polymers.[23] The vast majority of these investigations using PBC-DFT, however, has focused on homopolymers (or condensed polymers) (such as polyselenophenes, polythiophenes, etc).[20] Hence, for copolymers (or noncondensed polymers), such as these polymers used in this paper, the PBC-DFT approach may not be suitable and was not considered in this paper.

3.3. Design of Novel Polymers. Obviously, to improve the PCE of an organic solar cell, the band gap and HOMO energy level of a donor material should both be reduced. When coupled to $PC_{61}BM$ ($PC_{61}BM$, [6,6]-phenyl-C61-butynic acid methyl ester) as the acceptor moiety, a certain "ideal" conjugated donor polymer should exhibit a low HOMO energy level of −5.4 eV and a small band gap of 1.5 eV.[6] Many studies indicated that the LUMO energy level of D−A copolymers largely relies on the acceptor group.[47,48] The band gaps of these investigated polymers (1.85–2.02, 1.77–1.98, 1.82–1.97, and 1.92–2.04 eV for P1a, P2a, P3a, and P4a, respectively) are larger than 1.5 eV and are not in the optimal range. To obtain the polymers with lower band gaps and deeper LUMO energy levels, we hence use naphtho[1,2-c:5,6-c]bis[1,2,5]thiadiazole, a stronger electron-deficient acceptor, to replace 2,1,3-benzothiadiazole and construct four new polymers of P1b, P2b, P3b, and P4b. A similar strategy has been demonstrated recently by You et al.[48]

Figure 3 shows the optimized geometries of all these investigated monomers (at the PBE0/6-311G** level). The selected bond lengths (L) and dihedral angles (φ) of the monomers are listed in Table 4. The lengths of carbon−carbon single bonds (C−C) for M1a−M4b are all within 1.436−1.453 Å, which are shorter by ~0.1 Å than that of ethane (1.54 Å).
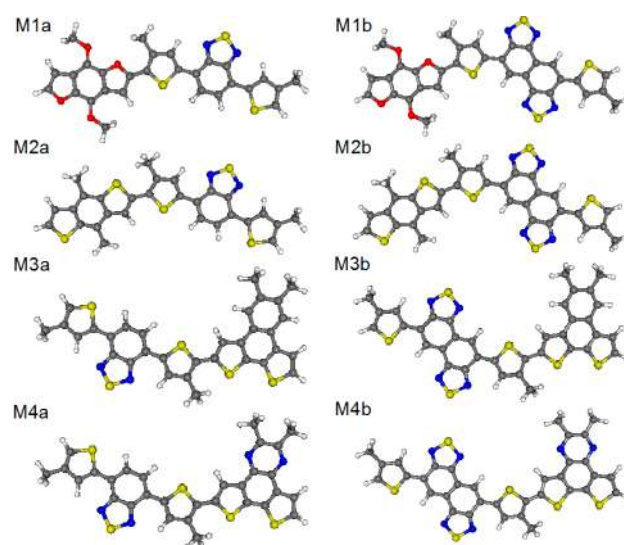
Figure 3. Optimized geometries of all investigated monomers calculated at the PBE0/6-311G** level. Color code: yellow (S), red (O), blue (N), black (C), and gray (H).

Table 4. Selected Bond Lengths (L, in Å) and Dihedral Angles (φ, in degree) of All These Monomers Calculated at the PBE0/6-311G Level**

oligomer	L_1	L_2	L_3	φ_1	φ_2	φ_3
M1a	1.436	1.448	1.452	0.1	0.2	0.6
M1b	1.436	1.448	1.453	1.9	0.6	1.4
M2a	1.446	1.449	1.452	28.2	7.0	4.2
M2b	1.446	1.450	1.453	29.2	8.6	7.6
M3a	1.444	1.449	1.452	26.5	7.3	5.5
M3b	1.444	1.449	1.453	26.1	9.4	7.1
M4a	1.444	1.449	1.452	27.3	7.6	5.3
M4b	1.444	1.449	1.453	25.7	9.3	7.3

This is partly caused by the π-bonding interaction and results in partial double-bond character on the bridge bond, thereby strengthening and shortening the bridge bond. The results demonstrate that the π-electrons are delocalized over the entire molecular framework rather than partially distributed on the donor or acceptor unit. The bridge bond (L_1, L_2, and L_3) lengths of M1b, M2b, M3b, and M4b (NT-based monomers) approximately equal those of the corresponding BT-based monomers (M1a, M2a, M3a, and M4a). This may be due to the fact that the NT unit contains a BT unit and leads to the same effect on the bridge band. The φ_1, φ_2, and φ_3 of M1a and M1b are all close to zero, which suggests that those monomers have good coplanar configurations. However, the dihedral angles in M2a and M2b are larger than those in M1a and M1b, respectively, although these molecules have similar backbones.

The possible reason is that the diameter of the oxygen atom in the BDF unit is smaller than those of the sulfur atoms in the other three units (BDT, NDT, and QDT) and results in a weak steric hindrance to adjacent units in the M1a and M1b which contain the BDF unit.[33]

We calculated the HOMO energy levels from DFT at the PBE0/6-311G** level on the monomer models of P1b−P4b, and the band gaps of P1b−P4b by TD-PBE0/6-311G**//PBE0/6-311G** approach on the dimer models. Figure 4 shows that the HOMO energy levels of P1b−P4b are
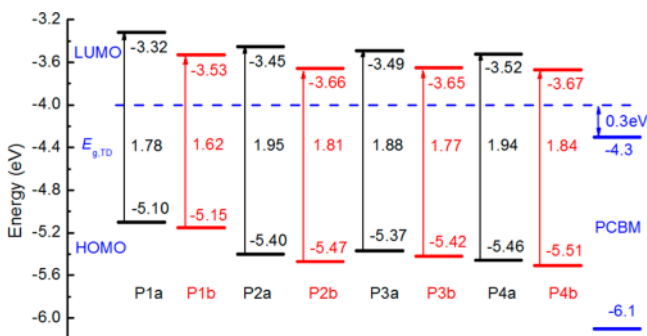

Figure 4. Frontier molecular orbital energy levels of P1a−P4b and PCBM.

−5.15, −5.47, −5.42, and −5.51 eV, respectively, and the band gaps of these polymers are 1.62, 1.81, 1.77, and 1.84 eV, respectively. The LUMO energy levels (−3.53, −3.66, −3.65, and −3.67 eV for P1b, P2b, P3b, and P4b, respectively) were estimated from the equation, $E_{LUMO} = E_{HOMO} + E_{g,TD}$. As expected, compared with the calculations of P1a−P4a, the band gaps of these newly designed polymers (P1b−P4b) are reduced by 0.16, 0.14, 0.11, and 0.10 eV, and the HOMO energy levels are slightly decreased by 0.05, 0.07, 0.05, and 0.05 eV. The results show that these designed polymers have narrower band gaps and lower HOMO energy levels than P1a−P4a and may possess larger J_{sc} and higher V_{oc} when applied to PSCs. In organic solar cells, $PC_{61}BM/PC_{71}BM$ ($PC_{71}BM$, [6,6]-phenyl-C71-butynic acid methyl ester) is widely used as the standard acceptor due to the relatively cheap price and commercial availability, although some other high performance C_{60}/C_{70} derivatives[8,49,50] have also been developed in the past years. Herein, we chose PCBM (PCBM, $PC_{61}BM/PC_{71}BM$) as the electron acceptor with the LUMO and HOMO energy levels of −4.3 and −6.1 eV, respectively.[3,10,48,51] The differences of LUMO energy levels between these newly designed donors (P1b−P4b) and the acceptor of PCBM are 0.77, 0.64, 0.65, and 0.63 eV, and all are larger than 0.3, which ensures efficient electron transfer from the donor to the acceptor.

Figure 5 shows the Frontier Molecular Orbitals (FMOs) for all the dimers (computed at the PBE0/6-311G** level). All HOMOs show the typical aromatic feature with electron delocalization for the whole conjugated dimers. On the contrary, in the case of LUMOs, electrons are withdrawn from the ring junctions and localized on the acceptor moieties. Moreover, as shown in Figure 5, the HOMOs possess bonding character within rings and antibonding character between consecutive subunits, while in the LUMOs there is inter-ring bonding and intraring antibonding.

In organic solar cells, typical ITO (indium tin oxide)/PEDOT:PSS or ITO/MoO₃ and LiF/Al or Ca/Al are considered to be suitable electrodes and are the most
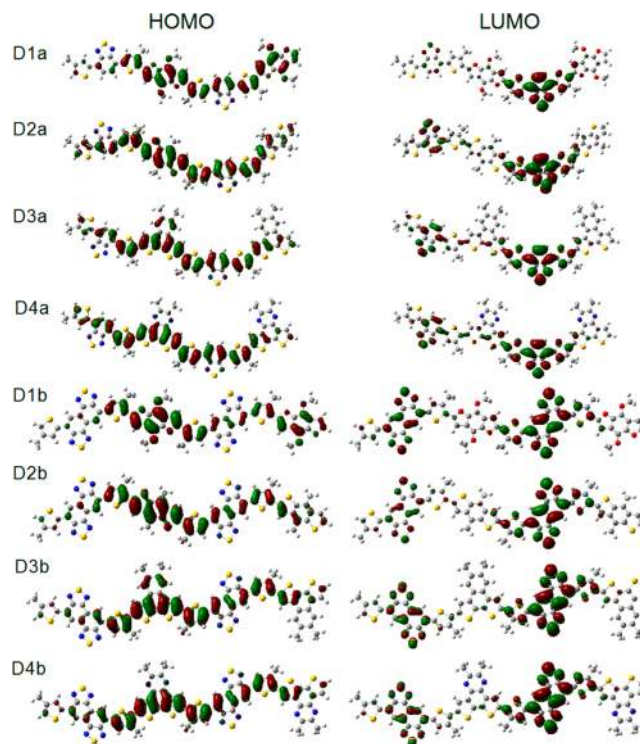

Figure 5. Electron density of HOMO and LUMO for all these dimers (D1a−D4b) computed at the PBE0/6-311G** level.

commonly used.[5,52,53] To evaluate the consistency of energy levels between the active layer (designed donors and the acceptor of PCBM) and electrodes, we assume the ITO/MoO₃ and LiF/Al are anode and cathode, respectively, in this case. Mihailetchi et al.[54] reported that there was no barrier energy for electron extraction between the LiF/Al electrode with $PC_{61}BM$ as an acceptor material. Generally, the Fermi energies of ITO/MoO₃ and LiF/Al are −4.7/−5.4 eV[51] and −4.3 eV,[55] respectively. According to the energy diagram of P1b−P4b, the HOMOs of these new polymers (−5.15, −5.47, −5.42, and −5.51 eV) are deeper than the Fermi energy level of ITO (−4.7 eV), and the LUMO of PCBM (−4.3 eV) is close to the Fermi energy level of LiF/Al (−4.3 eV), which means the energy levels of designed donors and acceptors match the corresponding Fermi energies of electrodes of ITO/MoO₃ and LiF/Al.

3.4. Absorption Spectra. The vertical singlet−singlet electronic transition energies and optical absorption spectra of all polymers (P1a−P4a and P1b−P4b) were calculated by the TD-PBE0/6-311G**//PBE0/6-311G** method with a dimer model. Figure 6 shows the simulated absorption spectra (considering the first 20 excited states), along with the absorption wavelength and oscillator strength (f). The calculated electronic transitions, oscillator strength ($f > 0.5$), and main configurations of all these dimers are also listed in Table 5.

The main transitions of all donors in the visible range correspond to the transitions from HOMO to LUMO, HOMO to LUMO + 2, and HOMO to LUMO + 4. The intramolecular charge transfer between electron-withdrawing groups (BT and NT) and the acceptor units results in the lowest-energy transitions (HOMO to LUMO). The calculated maximum absorption peaks (P1a: 698 nm, P2a: 637 nm, P3a: 659 nm, and P4a: 638 nm) are approximately consistent with the experiments (P1a: 613, ~670 nm,[33] P2a: ~625, ~700 nm,[34]
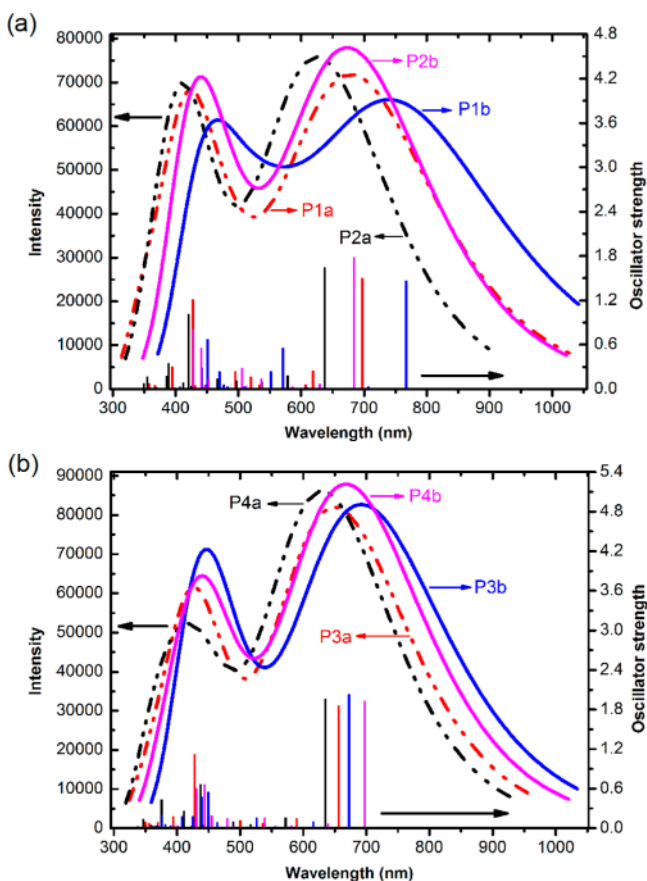
Figure 6. Comparison between the simulated absorption spectra and related oscillator strengths of the electronic transitions of (a) P1a, P2a, P1b, and P2b and (b) P3a, P4a, P3b, and P4b.

P3a: 629, 681 nm, and P4a: 609, 641 nm[35]). We further calculated the electronic transition energies and optical

absorption spectra of P1b−P4b by the same method as shown in Table 5 and Figure 6. The most intense absorption peaks for donors of P1b−P4b are about 767, 684, 699, and 675 nm, respectively, corresponding to the excitation energies ($E_{g,TD}$) of 1.62, 1.81, 1.77, and 1.84 eV. Compared to P1a−P4a, the absorption peaks of P1b−P4b become much broader and more intense within the visible and infrared region, which will facilitate more efficient sunlight absorption.

To estimate the properties of the designed molecules, we used the Scharber diagrams[10,14] to predict PCEs (%) of the solar cell combining those eight donors and PCBM. Using the design rules proposed by Scharber et al.,[10,14] which assumes a charge carrier mobility of 10^{-3} cm$^2 \cdot$V$^{-1} \cdot$S^{-1} and a fill factor (FF) of 0.65 (we cannot predict the fill factor of 0.65 from the first principles, and in real organic solar cells, the assumed FF is so large that it is usually difficult to achieve), one can predict the overall PCEs from the band gaps and the LUMO energy levels of the donors. The predictions (use the calculated results of $E_{g,TD}$ and LUMO energy levels) by the diagram show that the PCEs of eight solar cell devices made by P1a, P2a, P3a, P4a, P1b, P2b, P3b, P4b, and PCBM are ∼4%, ∼5%, ∼5%, ∼5%, ∼5%, ∼7%, ∼7%, and ∼7%, respectively. According to the results, the predicted PCE (∼4%) of P1a underestimates the experimental value[33] (5.0%) with an experiment FF of 0.55,[33] while the predicted PCEs (∼5%, ∼5%, ∼5%) of P2a, P3a, and P4a are in good agreement with these experimental data (5.0%,[34] 5.1%, 4.3%[35]). The predictions also show, compared with P1a−P4a, that P1b−P4b with the smaller band gaps and the lower LUMO energy levels exhibit the higher predicted PCEs of ∼5%, ∼7%, ∼7%, and ∼7% when used in combination with PCBM, respectively.

4. CONCLUSION

The methods of PBE0/6-311G** with a monomer model and TD-PBE0/6-311G**//PBE0/6-311G** with the dimer model have been used to theoretically investigate the electrical and the

Table 5. Calculated Electronic Transitions, Oscillator Strength ($f > 0.5$), and Main Configurations of All These Dimers by the TD-PBE0/6-311G//PBE0/6-311G** Approach**

	excitation energy		oscillator strength	main configuration	polymers $\lambda_{max,exp}$
	eV	nm			nm
D1a	1.78	698	1.50	HO → LU (69%)	613, ∼670[a]
	2.90	427	1.21	HO → LU + 2 (62%)	∼425[a]
D2a	1.95	637	1.64	HO → LU (68%)	∼625, ∼700[b]
	2.95	420	1.02	HO → LU + 2 (66%)	∼425[b]
D3a	1.88	659	1.86	HO → LU (68%)	629, 681[c]
	2.87	432	1.12	HO → LU + 2 (66%)	∼450[c]
D4a	1.94	638	1.96	HO → LU (68%)	609, 647[c]
	2.81	442	0.66	HO → LU + 2 (62%)	NA
D1b	1.62	767	1.46	HO → LU (69%)	
	2.17	571	0.55	HO − 2 → LU (65%)	
	2.75	451	0.67	HO → LU + 4 (52%)	-
D2b	1.81	684	1.78	HO → LU (68%)	-
	2.81	441	0.55	HO → LU + 3 (58%)	
	2.90	428	0.81	HO → LU + 4 (61%)	-
D3b	1.77	699	1.92	HO → LU (68%)	-
	2.77	448	0.66	HO → LU + 3 (57%)	-
	2.85	435	0.60	HO → LU + 4 (54%)	
D4b	1.84	675	2.03	HO → LU (67%)	-
	2.73	453	0.55	HO → LU + 2 (65%)	-

[a]From ref 33. [b]From ref 34. [c]From ref 35.

F

dx.doi.org/10.1021/jp306656c | J. Phys. Chem. C XXXX, XXX, XXX−XXX

optical features for a series of D−A conjugated polymers. The results show the methods we used in this paper reproduced very well the experimental HOMO energy levels and optical band gaps of P1a−P4a. The LUMO energy levels were appropriately calculated from the equation, $E_{LUMO} = E_{HOMO} + E_{g,TD}$, rather than from the less reliable LUMO eigenvalues. Compared with BT-based polymers of P1a−P4a, the newly designed NT-based polymers of P1b−P4b not only exhibit deeper HOMO levels but also possess smaller band gaps. The results also show that these newly designed polymers have the higher predicted PCEs of ∼5%, ∼7%, ∼7%, and ∼7%, respectively, when they are used in combination with PCBM as an acceptor.

■ AUTHOR INFORMATION

Corresponding Author
*Phone: 86-20-84727014. Fax: 86-20-84727014. E-mail: gaojw@scnu.edu.cn.

Notes
The authors declare no competing financial interest.

■ REFERENCES

(1) Yu, G.; Gao, J.; Hummelen, J. C.; Wudl, F.; Heeger, A. J. *Science* **1995**, *270*, 1789−1791.
(2) Günes, S.; Neugebauer, H.; Sariciftci, N. S. *Chem. Rev.* **2007**, *107*, 1324−1338.
(3) Chen, H. Y.; Hou, J.; Zhang, S.; Liang, Y.; Yang, G.; Yang, Y.; Yu, L.; Wu, Y.; Li, G. *Nat. Photonics* **2009**, *3*, 649−653.
(4) Huo, L.; Zhang, S.; Guo, X.; Xu, F.; Li, Y.; Hou, J. *Angew. Chem., Int. Ed.* **2011**, *123*, 9871−9876.
(5) Li, G.; Zhu, R.; Yang, Y. *Nat. Photonics* **2012**, *6*, 153−161.
(6) Zhou, H.; Yang, L.; You, W. *Macromolecules* **2012**, *45*, 607−632.
(7) Havinga, E.; Ten Hoeve, W.; Wynberg, H. *Synth. Met.* **1993**, *55*, 299−306.
(8) Li, Y. *Acc. Chem. Res.* **2012**, *45*, 723−733.
(9) Chochos, C. L.; Choulis, S. A. *Prog. Polym. Sci.* **2011**, *36*, 1326−1414.
(10) Scharber, M. C.; Mühlbacher, D.; Koppe, M.; Denk, P.; Waldauf, C.; Heeger, A. J.; Brabec, C. J. *Adv. Mater.* **2006**, *18*, 789−794.
(11) Thompson, B. C.; Fréchet, J. M. J. *Angew. Chem., Int. Ed.* **2008**, *47*, 58−77.
(12) He, Z.; Zhong, C.; Huang, X.; Wong, W.-Y.; Wu, H.; Chen, L.; Su, S.; Cao, Y. *Adv. Mater.* **2011**, *23*, 4636−4643.
(13) Blouin, N.; Michaud, A.; Gendron, D.; Wakim, S.; Blair, E.; Neagu-Plesu, R.; Belletête, M.; Durocher, G.; Tao, Y.; Leclerc, M. *J. Am. Chem. Soc.* **2008**, *130*, 732−742.
(14) Dennler, G.; Scharber, M. C.; Brabec, C. J. *Adv. Mater.* **2009**, *21*, 1323−1338.
(15) Seo, J. H.; Jin, Y.; Brzezinski, J. Z.; Walker, B.; Nguyen, T.-Q. *ChemPhysChem* **2009**, *10*, 1023−1027.
(16) Li, Z.; Lu, J.; Tse, S.-C.; Zhou, J.; Du, X.; Tao, Y.; Ding, J. *J. Mater. Chem.* **2011**, *21*, 3226−3233.
(17) Lin, L.-Y.; Lu, C.-W.; Huang, W.-C.; Chen, Y.-H.; Lin, H.-W.; Wong, K.-T. *Org. Lett.* **2011**, *13*, 4962−4965.
(18) Balan, B.; Vijayakumar, C.; Saeki, A.; Koizumi, Y.; Seki, S. *Macromolecules* **2012**, *45*, 2709−2719.
(19) Xiao, S.; Stuart, A. C.; Liu, S.; Zhou, H.; You, W. *Adv. Funct. Mater.* **2010**, *20*, 635−643.
(20) Pappenfus, T. M.; Schmidt, J. A.; Koehn, R. E.; Alia, J. D. *Macromolecules* **2011**, *44*, 2354−2357.
(21) Ku, J.; Lansac, Y.; Jang, Y. H. *J. Phys. Chem. C* **2011**, *115*, 21508−21516.
(22) Wang, X.; Sun, Y.; Chen, S.; Guo, X.; Zhang, M.; Li, X.; Li, Y.; Wang, H. *Macromolecules* **2012**, *45*, 1208−1216.
(23) Zade, S. S.; Zamoshchik, N.; Bendikov, M. *Acc. Chem. Res.* **2011**, *44*, 14−24.
(24) Yang, S.; Olishevski, P.; Kertesz, M. *Synth. Met.* **2004**, *141*, 171−177.
(25) Zhang, L.; Zhang, Q.; Ren, H.; Yan, H.; Zhang, J.; Zhang, H.; Gu, J. *Sol. Energy Mater. Sol. Cells* **2008**, *92*, 581−587.
(26) Zhou, H.; Yang, L.; Xiao, S.; Liu, S.; You, W. *Macromolecules* **2009**, *43*, 811−820.
(27) Jacquemin, D.; Perpète, E. A. *Chem. Phys. Lett.* **2006**, *429*, 147−152.
(28) Jacquemin, D.; Preat, J.; Wathelet, V.; Fontaine, M.; Perpète, E. A. *J. Am. Chem. Soc.* **2006**, *128*, 2072−2083.
(29) Jacquemin, D.; Perpète, E. A.; Scuseria, G. E.; Ciofini, I.; Adamo, C. *J. Chem. Theory Comput.* **2008**, *4*, 123−135.
(30) Wang, M.; Hu, X.; Liu, P.; Li, W.; Gong, X.; Huang, F.; Cao, Y. *J. Am. Chem. Soc.* **2011**, *133*, 9638−9641.
(31) Osaka, I.; Shimawaki, M.; Mori, H.; Doi, I.; Miyazaki, E.; Koganezawa, T.; Takimiya, K. *J. Am. Chem. Soc.* **2012**, *134*, 3498−3507.
(32) Osaka, I.; Abe, T.; Shimawaki, M.; Koganezawa, T.; Takimiya, K. *ACS Macro Lett.* **2012**, *1*, 437−440.
(33) Huo, L.; Huang, Y.; Fan, B.; Guo, X.; Jing, Y.; zhang, M.; Li, Y.; Hou, J. *Chem. Commun.* **2012**, *48*, 3318−3320.
(34) Zhou, H.; Yang, L.; Stuart, A. C.; Price, S. C.; Liu, S.; You, W. *Angew. Chem., Int. Ed.* **2011**, *123*, 3051−3054.
(35) Zhou, H.; Yang, L.; Liu, S.; You, W. *Macromolecules* **2010**, *43*, 10390−10396.
(36) Frisch, M. J.; Trucks, G. W.; Schlegel, H. B.; Scuseria, G. E.; Robb, M. A.; Cheeseman, J. R.; Montgomery, J. A.; Jr.; Vreven, T.; Kudin, K. N.; Burant, J. C.; et al. *Gaussian 03*, Revision B.05; Gaussian, Inc.: Pittsburgh PA, 2003.
(37) Runge, E.; Gross, E. K. U. *Phys. Rev. Lett.* **1984**, *52*, 997−1000.
(38) Perdew, J. P. *Phys. Rev. B* **1986**, *33*, 8822−8824.
(39) Becke, A. D. *Phys. Rev. A* **1988**, *38*, 3098−3100.
(40) Lee, C.; Yang, W.; Parr, R. G. *Phys. Rev. B* **1988**, *37*, 785−789.
(41) Adamo, C.; Barone, V. *J. Chem. Phys.* **1999**, *110*, 6158−6170.
(42) Becke, A. D. *J. Chem. Phys.* **1993**, *98*, 1372−1377.
(43) Casida, M. E.; Jamorski, C.; Casida, K. C.; Salahub, D. R. *J. Chem. Phys.* **1998**, *108*, 4439−4449.
(44) Stratmann, R. E.; Scuseria, G. E.; Frisch, M. J. *J. Chem. Phys.* **1998**, *109*, 8218−8224.
(45) Hirata, S.; Head-Gordon, M. *Chem. Phys. Lett.* **1999**, *302*, 375−382.
(46) Burke, K.; Werschnik, J.; Gross, E. K. U. *J. Chem. Phys.* **2005**, *123*, 062206.
(47) Zhou, H.; Yang, L.; Stoneking, S.; You, W. *ACS Appl. Mater. Interfaces* **2010**, *2*, 1377−1383.
(48) Zhou, H.; Yang, L.; Price, S. C.; Knight, K. J.; You, W. *Angew. Chem., Int. Ed.* **2010**, *122*, 8164−8167.
(49) Kim, K.-H.; Kang, H.; Nam, S. Y.; Jung, J.; Kim, P. S.; Cho, C.-H.; Lee, C.; Yoon, S. C.; Kim, B. J. *Chem. Mater.* **2011**, *23*, 5090−5095.
(50) Zhang, C.; Chen, S.; Xiao, Z.; Zuo, Q.; Ding, L. *Org. Lett.* **2012**, *14*, 1508−1511.
(51) Sun, Y.; Welch, G. C.; Leong, W. L.; Takacs, C. J.; Bazan, G. C.; Heeger, A. J. *Nat. Mater.* **2011**, *11*, 44−48.
(52) Li, X.; Sha, W. E. I.; Choy, W. C. H.; Fung, D. D. S.; Xie, F. *J. Phys. Chem. C* **2012**, *116*, 7200−7206.

(53) Peters, C. H.; Sachs-Quintana, I. T.; Mateker, W. R.; Heumueller, T.; Rivnay, J.; Noriega, R.; Beiley, Z. M.; Hoke, E. T.; Salleo, A.; McGehee, M. D. *Adv. Mater.* **2012**, *24*, 663−668.

(54) Mihailetchi, V. D.; Blom, P. W. M.; Hummelen, J. C.; Rispens, M. T. *J. Appl. Phys.* **2003**, *94*, 6849−6854.

(55) Eo, Y. S.; Rhee, H. W.; Chin, B. D.; Yu, J. W. *Synth. Met.* **2009**, *159*, 1910−1913.

H

dx.doi.org/10.1021/jp306656c | *J. Phys. Chem. C* XXXX, XXX, XXX−XXX